Light-induced dynamics in the Lorentz oscillator model with magnetic forces

W. M. Fisher[*] and S. C. Rand

Applied Physics Program, University of Michigan, Ann Arbor, Ann Arbor, Michigan 48109, USA
(Received 6 October 2009; published 2 July 2010)

The classical Lorentz oscillator model of bound electron motion ordinarily excludes magnetic forces at nonrelativistic intensities for the simple reason that their magnitude is small. However, perturbative and numerical results show that when the $\vec{v} \times \vec{B}$ term is retained, dynamically enhanced terms give rise to large amplitude, magnetically induced charge displacements at zero frequency and at twice the driving frequency in the Cartesian laboratory frame. Numerical simulations of electron motion are in accord with the predictions of perturbative theory for steady-state motion in the classical picture. Direct integration shows that magnetic response which is comparable to electric dipole response can arise in transparent dielectrics at optical frequencies. Parametric instability in the equations of motion is implicated as the source of rapid energy transfer from electric to magnetic motions by reduction of the equations to a complex Mathieu equation.

I. INTRODUCTION

Recent experiments have shown that large magnetic dipole response is observed in transparent dielectric materials at light intensities far below the threshold for relativistic electron motion [1,2]. Classical steady-state analysis reveals that a nonlinear mechanism exists that can account for the large induced magnetic susceptibility [2]. A quantum-mechanical analysis, valid near resonances, has also been published that agrees with the classical theory and achieves quantitative agreement with experimental results for the ratio of electric to magnetic signals [3]. Here, the results of classical perturbation analysis and numerical integration of the equations of motion give independent corroboration and important perspective regarding the mechanism of these surprising effects. Qualitative predictions of perturbation analysis are exhaustively checked by numerical simulation. The frequency and intensity requirements for efficient energy transfer between electric and magnetic degrees of freedom driven by light are examined using the energy-rate method [4]. Finally, the equations of motion are shown to reduce to a complex Mathieu equation. These results, combined with previous work, predict that charge excursions perpendicular to E, driven by the field product EB, can be half as large as motion parallel to E, enhanced by a factor associated with parametric resonance.

II. LORENTZ OSCILLATOR MODEL

The Lorentz oscillator model (LOM), which is an important paradigm of classical optics, is based on a picture in which an electron is bound to the nucleus by a harmonic potential and undergoes forced motion subject to damping [5]. The driving forces are due to external electromagnetic fields which set the electron into motion according to the equation,

$$\ddot{\vec{r}} + \gamma\dot{\vec{r}} + \omega_0^2\vec{r} = \frac{q}{m}(\vec{E} + \dot{\vec{r}} \times \vec{B}), \qquad (1)$$

where $\vec{r}$ is the relative position vector from the nucleus to the electron, γ is the phenomenological damping coefficient, ω_0

is the natural frequency, q is the charge of the electron, and m is the mass of the electron. In the most general case the $\vec{E}$ and $\vec{B}$ fields are both functions of time and space. The case of interest here is that of a monochromatic electromagnetic plane wave interacting with an atom in otherwise free space. The relative field amplitudes then obey the well-known relationship $|\vec{B}| = |\vec{E}|/c$, allowing us to write the equation of motion as

$$\ddot{\vec{r}} + \gamma\dot{\vec{r}} + \omega_0^2\vec{r} = \frac{q}{m}\left(\vec{E} + \frac{\dot{\vec{r}}}{c} \times \hat{k} \times \vec{E}\right). \qquad (2)$$

The magnitude of the magnetic force, given by the second term in parentheses in Eq. (2) varies as $\dot{r}/c$. The electron velocities achievable during a half-cycle of the driving field from moderately intense sources are small ($v/c \ll 1$). Therefore, the magnetic forcing term appears to be negligible and is typically dropped from the analysis for light fields that are "nonrelativistic" ($I \ll 10^{18}$ W/cm^2). This reduces the LOM to a form with only the dominant electric field as a driving force:

$$\ddot{\vec{r}} + \gamma\dot{\vec{r}} + \omega_0^2\vec{r} = \frac{q}{m}\vec{E}. \qquad (3)$$

In this paper, the arguments previously mentioned not withstanding, we retain the magnetic force and explore the dynamics of the LOM with all its forcing terms. To begin, we use the vector identity $\vec{a} \times \vec{b} \times \vec{c} = (\vec{a} \cdot \vec{c})\vec{b} - (\vec{a} \cdot \vec{b})\vec{c}$ to rewrite the forcing terms in Eq. (2) in the form,

$$\ddot{\vec{r}} + \gamma\dot{\vec{r}} + \omega_0^2\vec{r} = \frac{q}{m}\left(\vec{E} + \frac{1}{c}[(\dot{\vec{r}} \cdot \vec{E})\hat{k} - (\dot{\vec{r}} \cdot \hat{k})\vec{E}]\right), \qquad (4)$$

following Ref. [6]. The direction of propagation $\hat{k}$ is chosen to be along the $\hat{z}$ direction and the polarization to be along $\hat{x}$. In these coordinates, the general equation of motion (4) reduces to the two coupled differential equations,

$$\ddot{x} + \gamma_x\dot{x} + \omega_x^2 x = \frac{qE_0}{m}\cos(\omega t) - \frac{qB_0}{m}\cos(\omega t)\dot{z}, \qquad (5)$$

$$\ddot{z} + \gamma_z\dot{z} + \omega_z^2 z = \frac{qB_0}{m}\cos(\omega t)\dot{x}, \qquad (6)$$

where the magnetic field amplitude has been reinserted. The damping coefficients and natural frequencies have been

---

*wfisher@umich.edu

permitted to assume different values in orthogonal directions. In a departure from earlier work [6], these equations will be considered in component form to avoid inadvertent omission of any terms that couple motion between the x and z directions. Furthermore, the last driving term on the right-hand side of each equation, which contains the factor B_0, will be evaluated using $B_0 = E_0/c$ allowing us to consider the magnetic driving forces as a perturbation of the dominant electric driving force for all intensities of the driving field. We now proceed to solve the system of differential Eqs. (5) and (6) using a regular perturbation expansion in powers of B_0 [7].

III. PERTURBATION SOLUTION

Since the magnetic field terms in Eqs. (5) and (6) are small compared to the electric field terms, they can be considered a perturbation of the motion. Introducing an order parameter λ, the solutions are therefore assumed to take the form,

$$x(t) = x_0(t) + \lambda x_1(t) + \lambda^2 x_2(t) + \cdots \quad (7)$$

$$z(t) = z_0(t) + \lambda z_1(t) + \lambda^2 z_2(t) + \cdots, \quad (8)$$

where $x_1, x_2, \ldots$ are amplitudes of motion along $\hat{x}$ associated with orders $1, 2, \ldots$. In the present treatment the electric field is introduced in zero order and the magnetic field is considered in higher orders. Substituting Eqs. (7) and (8) into the equations of motion and collecting terms of like order, we proceed in the standard iterative fashion.

A. Zeroth order

Collecting terms that are zeroth order in λ, one finds

$$\ddot{x}_0 + \gamma_x \dot{x}_0 + \omega_x^2 x_0 = \frac{qE_0}{m} \cos(\omega t), \quad (9)$$

$$\ddot{z}_0 + \gamma_z \dot{z}_0 + \omega_z^2 z_0 = 0. \quad (10)$$

These equations of motion constitute the standard LOM and are well studied. For an electron initially at rest at the origin, they yield the solutions,

$$x_0(t) = \frac{qE_0}{m\sqrt{\left[\left(\omega_x^2 - \omega^2\right)^2 + \gamma_x^2 \omega^2\right]}} \cos(\omega t + \phi_0), \quad (11)$$

$$z_0(t) = 0, \quad (12)$$

where $\phi_0 = \tan^{-1}\left(\frac{-\gamma_x \omega}{(\omega_x^2 - \omega^2)}\right)$. The solution for motion along the electric field is proportional to the amplitude of the applied field E_0 and oscillates harmonically at the driving frequency ω. The amplitude is enhanced near resonance by a factor that depends on the detuning, $(\omega_x - \omega)$, and the damping, γ_x, of the linear motion along $\hat{x}$.

B. First order

Terms that are first order in λ yield the equations,

$$\ddot{x}_1 + \gamma_x \dot{x}_1 + \omega_x^2 x_1 = -\frac{qB_0}{m} \cos(\omega t) \dot{z}_0, \quad (13)$$

$$\ddot{z}_1 + \gamma_z \dot{z}_1 + \omega_z^2 z_1 = \frac{qB_0}{m} \cos(\omega t) \dot{x}_0. \quad (14)$$

The driving terms of these equations depend on the time derivatives of the zeroth-order solutions.

$$\dot{x}_0 = -\frac{\omega qE_0}{m\sqrt{\left[\left(\omega_x^2 - \omega^2\right)^2 + \gamma_x^2 \omega^2\right]}} \sin(\omega t + \phi_0), \quad (15)$$

$$\dot{z}_0 = 0. \quad (16)$$

To solve the system of Eqs. (13)–(16), the homogeneous version of the x_1 equation is considered first.

$$\ddot{x}_1 + \gamma_x \dot{x}_1 + \omega_x^2 x_1 = 0. \quad (17)$$

The solution to this equation with our initial conditions is simply

$$x_1(t) = 0. \quad (18)$$

Equation (18) confirms the expected result that there is no additional response in the x direction at first order.

The z_1 equation is solved next. The homogeneous solution is the same as the previous order, so only the particular solution needs to be found. Substituting (15) into (14), one finds

$$\ddot{z}_1 + \gamma_z \dot{z}_1 + \omega_z^2 z_1 = -\frac{\omega q^2 E_0 B_0}{m^2 \sqrt{\left[\left(\omega_x^2 - \omega^2\right)^2 + \gamma_x^2 \omega^2\right]}}$$
$$\times \cos(\omega t)\sin(\omega t + \phi_0), \quad (19)$$

in which a product of sine and cosine functions at the optical frequencies appears. Using the trigonometric identity $\cos(a)\sin(b) = \frac{1}{2}[\sin(a+b) - \sin(a-b)]$ this may be simplified to

$$\ddot{z}_1 + \gamma_z \dot{z}_1 + \omega_z^2 z_1 = -\frac{\omega q^2 E_0 B_0}{2m^2 \sqrt{\left[\left(\omega_x^2 - \omega^2\right)^2 + \gamma_x^2 \omega^2\right]}}$$
$$\times [\sin(2\omega t + \phi_0) - \sin(\phi_0)]. \quad (20)$$

Because this equation is linear, a particular solution of the entire equation of motion for $z(t)$ can be found by analyzing each of the two driving terms in square brackets on the right side of (20) separately and then adding the results. The solution for $z(t)$, complete to first order, is

$$z(t) = z_1(0,t) + z_1(2\omega,t)$$
$$= \frac{-\omega q^2 E_0 B_0}{2m^2 \omega_z^2 \sqrt{\left(\omega_x^2 - \omega^2\right)^2 + \gamma_x^2 \omega^2}} \sin(\phi_0) \quad (21)$$
$$+ \frac{1}{\sqrt{\left[\omega_z^2 - (2\omega)^2\right]^2 + \gamma_z^2 (2\omega)^2}}$$
$$\times \frac{\omega q^2 E_0 B_0}{2m^2 \sqrt{\left(\omega_x^2 - \omega^2\right)^2 + \gamma_x^2 \omega^2}} \sin(2\omega t + \phi_0 - \phi_1),$$
$$\quad (22)$$

where $\phi_1 = \tan^{-1}\left(\frac{-\gamma_z 2\omega}{[\omega_z^2 - (2\omega)^2]}\right)$. Similarly, the solution for $x(t)$, correct to first order, is

$$x(t) = x_0(\omega,t)$$
$$= \frac{qE_0}{m\sqrt{\left[\left(\omega_x^2 - \omega^2\right)^2 + \gamma_x^2 \omega^2\right]}} \cos(\omega t + \phi_0). \quad (23)$$

The first-order solution for $x_1(t)$ is unchanged with respect to the linear response expression for $x_0(t)$. Hence, it still shows a linear dependence on the input field, together with damped resonance about the natural frequency ω_x and a damping-dependent phase shift ϕ_0. The motion in the z direction, given by $z_1(t)$, is much more complicated. First, there are two different frequency components in the response, one at zero frequency and another that oscillates at twice the driving frequency. However, both components show a quadratic dependence on the input fields as is expected for a magneto-optic nonlinearity. Both terms also show a resonance at the natural frequency ω_x, but the second, frequency-doubled 2ω term shows an additional resonance at $\omega = \omega_z/2$. Equations (23) and (22) are the main analytic results of this paper.

IV. NUMERICAL STUDIES

In this section, a numerical technique is used to check results from the perturbation theory of Sec. III both on and off resonance. Generally speaking, agreement between numerical integration of the equations of motion and perturbative predictions is not expected since perturbation theory is not strictly valid under resonant conditions. Its failure is due not merely to the appearance of a pole on resonance (since this shortcoming can be remedied by the introduction of damping) but to formal nonconvergence of the perturbation expansion. High-order terms in the expansion cannot be overlooked on resonance. Physically, the simple picture of perturbation theory fails in resonant light-matter interactions because multiphoton interactions become possible and resonant optical excitations also alter the electronic structure of the atoms themselves via the AC Stark effect [8]. However, the changes effected by higher-order terms and interactions have little impact on the absorption or dispersion of a single beam when the Rabi frequency ($\Omega = \mu E_0/\hbar$) is far less that the transition frequency ω_0. Under these conditions, both the LOM and perturbation theory accurately describe the main features of real atoms both on and off resonance, treating the damping constants as adjustable parameters. Hence, the objective here is to check the main features of the perturbative model using numerical integration and to confirm that inclusion of magnetic forces in the LOM is essential for the description of optically driven magnetic response of bound electrons at intermediate (but nonrelativistic) intensities.

The perturbation solutions given by (22) and (23) can be checked by comparing their predictions to numeric solutions. Using a fourth-order Runge-Kutta integration method, Eqs. (5) and (6) are solved and the motion of the electron is plotted to examine transient and steady-state response. Figure 1 is a reference plot showing the position of the electron plotted with all parameters set to unity except B_0, which is set to $1/(3 \times 10^8)$ to preserve the ratio $B_0/E_0 = 1/c$ of a plane wave. Thus, the electric field amplitude is $E_0 = 1$ V/m. In Fig. 1, both the x and z motions reach steady-state oscillation after a short transient period. The period of the x motion in Fig. 1 is 2π and the period of the z motion in Fig. 1 is π. Hence, the frequency ratio is $1/2$, as predicted in the perturbation result of Eq. (22). It can also be seen that the x motion is centered about zero, whereas the z motion is offset by a constant amount in the steady state as predicted
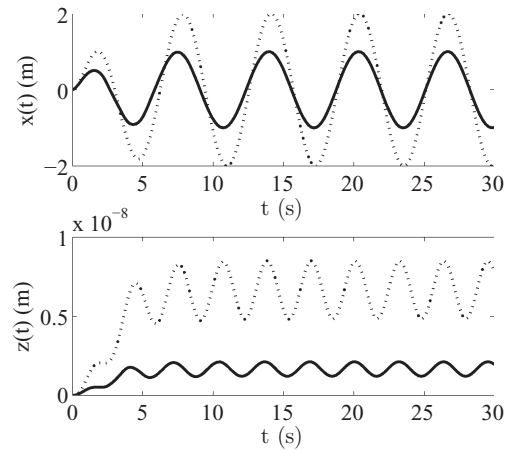
FIG. 1. Solid lines are reference plots of electron motion with all parameters set to unity while preserving $E_0 = 1$ V/m and $B_0 = 1/c$ T. Dashed lines are plots of electron motion with the fields doubled to $E_0 = 2$ V/m and $B_0 = 2/c$ T.

by the zero frequency term of the perturbation solution. While the amplitude of motion at low intensity is nine orders of magnitude greater in the x direction than in the z direction, the amplitude of motion along these two directions becomes comparable at higher intensity ($E_0 = 10^8$ V/m; $B_0 = 10^8/c$ T) as seen in Fig. 2.

Numerous additional checks of the perturbation solution and its predictions were made using this method of numerical integration of the equations of motion. For this purpose, a single parameter in Eqs. (22) and (23) was chosen and all other parameters were fixed at their reference value. The chosen parameter was then varied over a wide range of values and the steady-state values of the x amplitude, z amplitude, and the z offset were plotted versus the parameter. In Figs. 3–5, projections of electron trajectories on the laboratory x and z axes are computed by direct integration of these force equations and amplitudes of motion along these two axes are plotted as a function of field intensity and natural oscillation frequency for comparison with (22) and (23). As an example, the solid curves in Fig. 1 were calculated with all parameters
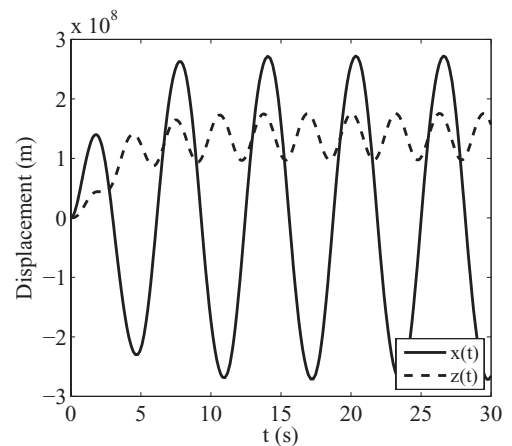
FIG. 2. Plots of electron motion in both x and z directions on the same scale for all parameters set to unity while $E_0 = 10^8$ V/m and $B_0 = 10^8/c$ T.
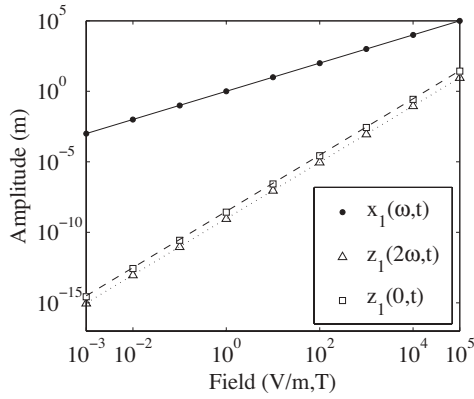
FIG. 3. Behavior of x and z amplitudes and z offset versus the input field. All parameters fixed at unity *except* E_0 and B_0 which are varied to generate the plot. Note that the x amplitude shows a linear dependence on field whereas the z amplitude and offset both exhibit quadratic dependencies.

(except E_0 and B_0) set to the default value of unity. The dashed curves were obtained by doubling the values of E_0 and B_0. Clearly the x amplitude in Fig. 1 increases linearly with field amplitude, but both the z offset and z amplitude increase quadratically. This procedure was repeated for a wide range of values of E_0 and B_0 to generate Fig. 3. The resulting log-log plot shows that the amplitude of the x motion grows linearly with increasing field. The slope of the fitted curve is one. The amplitude of z motion and the offset of z motion increase quadratically with the field. The slopes of their fitted curves are both two.

Figure 4 shows that both z amplitude and z offset have a resonance at $\omega_x = 1$ as predicted by the perturbation solution. The x amplitude also has a resonance at $\omega_x = 1$ but this result was not included in the figure because it is predicted by the standard LOM. Figure 5 shows that the z amplitude has a resonance at $\omega_z = 2$ as predicted by the perturbation solution. It also shows that the z offset obeys a $1/\omega_z^2$ dependence, indicated by the slope of -2. Thus, all of the major features of response amplitude predicted by the perturbation calculation are confirmed by numeric integration of the equations of motion.
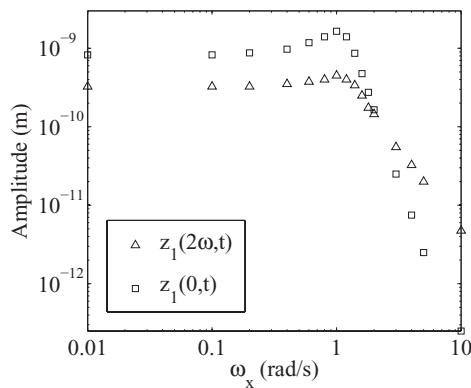
FIG. 4. Behavior of z amplitude and z offset versus ω_x. All parameters fixed at unity *except* ω_x which is varied to generate the plot. Note that both have a resonance at $\omega_x = 1$.
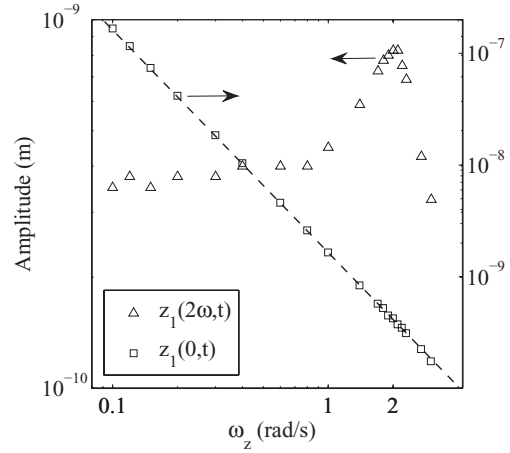
FIG. 5. Behavior of z amplitude and z offset versus ω_z. All parameters fixed at unity *except* ω_z which is varied to generate the plot. Note that the z amplitude has a resonance at $\omega_z = 2$ and that the z offset follows an inverse quadratic behavior (slope $= -2$).

V. PARAMETRICALLY ENHANCED DYNAMICS

In Sec. IV it was shown that charge motion induced by an incident plane wave is no longer linear when magnetic forces are included. In particular, motion along the direction of propagation is much larger at higher intensities than expected due to magnetic coupling between the motion in the x and z directions. Even though the coupling strength is dependent on the magnetic field amplitude, which is small compared to the electric field amplitude, it is evident that large amplitude, complex dynamics which are magnetic in origin arise at moderate field strengths. In the remainder of this paper the origin of large-amplitude magnetic dynamics at nonrelativistic intensities is clarified.

By rearranging Eqs. (5) and (6) into a form so that all terms that depend on the coordinates are on the left-hand side and the external driving terms are on the right-hand side, the underlying structure can be more clearly seen.

$$\ddot{x} + \gamma_x \dot{x} + \frac{qB_0}{m}\cos(\omega t)\dot{z} + \omega_x^2 x = \frac{qE_0}{m}\cos(\omega t), \quad (24)$$

$$\ddot{z} + \gamma_z \dot{z} - \frac{qB_0}{m}\cos(\omega t)\dot{x} + \omega_z^2 z = 0. \quad (25)$$

The nonautonomous terms whose coefficients depend on the independent variable t are of main interest here. All terms in Eqs. (24) and (25) have constant coefficients except for the coupling terms. The Lorentz force terms add to the equations an effective sinusoidal, time-varying damping coefficient. Equations with sinusoidallyvarying coefficients are of particular interest in the study of instability and it is this aspect of the equations that is of particular interest here [9].

To set the discussion of instabilities in appropriate context, we briefly review dynamics described by the Mathieu equation. The Mathieu equation is a simple model for a classic problem in instability, namely the vertically driven pendulum. In the prototypical problem, a rigid, massless rod is fixed to a pivot at one end and a mass at the other. The fixed point is then moved vertically, sinusoidally at some amplitude. The

linearized equation of motion of the pendulum can then be reduced to

$$\frac{d^2u}{dt^2} + [a - b\cos(2t)]u = 0. \tag{26}$$

The sinusoidally time-dependent spring constant, known as the "parametric excitation," acts as an energy source causing the amplitude of motion, u, to grow to a value dependent on the values a and b. For certain values of a and b, the amplitude of the pendulum grows exponentially to infinity. These regions are said to undergo unstable motion because they are in parametric resonance. More discussion of this topic can be found in many differential equation texts, including [9], [10]. For an intuitive introduction, see Ref. [11].

In the case of the vertically driven pendulum, the system spends more time in unstable motion as the amplitude of the parametric excitation grows. The addition of damping does not remove the regions of instability, though it does make them smaller. Only nonlinearities in the system formally prevent the amplitude from growing to infinity exponentially. For sufficiently large amplitude motion it should be admitted, however, that the Mathieu differential equation ceases to be the equation of motion since the approximation of a harmonic restoring force eventually breaks down. Ionization is one way that breakdown of this kind can occur in our system of interest.

For the LOM augmented by magnetic forces, it was shown in Sec. IV that z motion is enhanced dynamically by eight orders of magnitude at moderate intensities. We now turn to an examination of predictions for parametrically resonant stable and unstable motions in this model. For ease of mathematical analysis, we use dimensionless forms of the complete equations of motion (5) and (6) with the substitutions $x \rightarrow \chi$, $z \rightarrow \zeta$, and $t \rightarrow \tau$:

$$\frac{d^2\chi}{d\tau^2} + \frac{\gamma_x}{\omega}\frac{d\chi}{d\tau} + \frac{\omega_x^2}{\omega^2}\chi = \cos(\tau) - \frac{qB_0}{m\omega}\cos(\tau)\frac{d\zeta}{d\tau}, \tag{27}$$

$$\frac{d^2\zeta}{d\tau^2} + \frac{\gamma_z}{\omega}\frac{d\zeta}{d\tau} + \frac{\omega_z^2}{\omega^2}\zeta = \frac{qB_0}{m\omega}\cos(\tau)\frac{d\chi}{d\tau}, \tag{28}$$

which contain the following constants:

$$a = \frac{\gamma_x}{\omega}; \quad b = \frac{\omega_x^2}{\omega^2}; \quad c = \frac{\gamma_z}{\omega}; \quad d = \frac{\omega_z^2}{\omega^2}; \quad e = \frac{qB_0}{m\omega}. \tag{29}$$

The constants a and c represent dimensionless damping parameters, b and d represent dimensionless natural frequencies, and e represents the dimensionless cyclotron frequency due to the magnetic field of the incident plane wave. First, consider a spherically symmetric molecule in which the x and z directions are equivalent, resulting in $a = c$ and $b = d$. For ease of interpretation, these constants may be redefined with symbols that are in standard use, namely,

$$\gamma = a = c, \tag{30}$$

$$\omega^2 = b = d, \tag{31}$$

$$f_c = e, \tag{32}$$

where we now refer to γ as the dimensionless damping constant, ω as the dimensionless natural frequency, and f_c as the dimensionless cyclotron frequency.
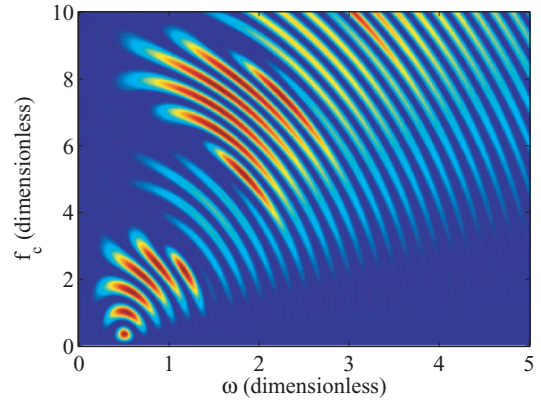
FIG. 6. (Color online) Energy transfer diagram of parameter space for the complex Mathieu equation (37) evaluated over a 6π integration period using the energy-rate Method. Red areas (lighter finger structure) indicate rapid transfer of energy from x (electric) to z (magnetic) degrees of freedom. Blue areas (dark) indicate no energy transfer.

The equations of motion then take on the dimensionless form,

$$\frac{d^2\chi}{d\tau^2} + \gamma\frac{d\chi}{d\tau} + \omega^2\chi = \cos(\tau) - f_c\cos(\tau)\frac{d\zeta}{d\tau}, \tag{33}$$

$$\frac{d^2\zeta}{d\tau^2} + \gamma\frac{d\zeta}{d\tau} + \omega^2\zeta = f_c\cos(\tau)\frac{d\chi}{d\tau}. \tag{34}$$

In order to determine the stability or instability of the motion we need only the terms that depend on the coordinates [9]. Dropping the $\cos(\tau)$ factor, which is an external forcing term (i.e., it does not depend on the coordinates of the system), Eq. (33) reduces to

$$\frac{d^2\chi}{d\tau^2} + \gamma\frac{d\chi}{d\tau} + \omega^2\chi = -f_c\cos(\tau)\frac{d\zeta}{d\tau}, \tag{35}$$

and Eq. (34) undergoes no change. To proceed, we first make use of the energy-rate method [4] to plot an energy transfer diagram of the dimensionless system of equations as shown in Fig. 6. Wide regions of parameter space are shown to couple energy between the x and z directions of motion.

Second, Eqs. (34) and (35) can be combined into a single complex equation of motion of the variable $y = (\chi + i\zeta)$. Multiplying Eq. (34) by i, adding it to Eq. (35), and collecting terms results in a single, sinusoidally damped oscillator equation.

$$\frac{d^2y}{d\tau^2} + [\gamma - if_c\cos(\tau)]\frac{dy}{d\tau} + \omega^2 y = 0. \tag{36}$$

The stability of the Mathieu equation itself is well studied, so a key result of the present work is that this equation can be rewritten in the form of a Mathieu equation. By comparing (36) and (26) it is clear that the damping terms must be eliminated for them to be formally identical. Mathematically, this may be done by modifying (36) with an integral transformation [12]. The transformed variable $W(t)$ is defined according to the expression $y(t) = W(t)e^{\frac{1}{2}\int_0^t[\gamma - if_c\cos(\tau)]d\tau}$. Substituting this into

the complex equation of motion and collecting terms, one finds

$$\ddot{W}(t) + \frac{1}{8}\{-2\gamma^2 + 8\omega^2 + f_c^2 + 4if_c[\gamma\cos(t) - \sin(t)]$$
$$+ f_c^2\cos(2t)\}W(t) = 0. \tag{37}$$

This is a Mathieu-type equation of the complex variable $W(t)$. The quantity $\frac{1}{8}(-2\gamma^2 + 8\omega^2 + f_c^2)$ acts as the Mathieu constant a and the quantity $\frac{1}{8}f_c^2$ acts as the Mathieu constant b. The successful transformation of the complete Lorentz oscillator model to a Mathieu-type differential equation confirms that it supports complex dynamics. In particular, the electric and magnetic degrees of freedom of the system can exchange energy due to the magnetic modulation at doubled frequency $2t$ that is governed by the constant f_c (Fig. 6).

It should be noted that the quantity f_c which represents the Lorentz force strength appears in all time-dependent coefficients of the equation indicating that it is the source of unexpected, magnetically induced behavior. If f_c were zero, as applicable to the customary LOM, the equations of motion could not be written as a Mathieu-type differential equation. On the other hand, the imaginary, sinusoidal, time-dependent excitation terms in Eq. (37) appear to offer novel degrees of freedom and dynamic behavior worthy of additional study.

VI. CONCLUSION

The theoretical results based on perturbative solution of Eqs. (5) and (6) have revealed a second-order magneto-electric process leading to charge separation and doubled-frequency motion along the direction of propagation of linearly polarized light. These effects correspond to static and second harmonic polarizations of the medium driven by the product of electric and magnetic field amplitudes. Classically, these phenomena can take place in the presence of inversion symmetry, making them different from previous quadratic optical nonlinearities requiring noncentrosymmetric media. Hence, their results predict previously unknown nonlinear optical effects that appear as the result of Lorentz forces exerted by light.

Their quantum-mechanical implications have been analyzed in Ref. [3].

The results have been verified by numerical integration and show that at nonrelativistic intensities, after a short transient period, a steady driving field establishes sinusoidal motion at the fundamental frequency ω along the electric field axis $\hat{x}$ and at 2ω in the longitudinal direction $\hat{z}$. The longitudinal oscillation reflects motion on a circular arc in the x-z plane. The amplitude of motion along $\hat{x}$ is linear with respect to the input intensity, as expected, whereas the amplitude of both the motion and the offset along $\hat{z}$ is quadratic versus input intensity. The magnitude of excursions along $\hat{z}$ can be quite large at moderate intensities and both amplitudes show the predicted resonant behavior. In particular, magnetically induced charge oscillations can have an amplitude comparable to the electric response when the optical intensity is still 10 orders of magnitude below the relativistic threshold (Fig. 2). This result is very unexpected [13], but agrees with recent experiments [1,2]. At intensities above those which yield saturated magnetic response, more complex dynamics can be expected.

As shown in Fig. 4, induced charge motions in all directions exhibit resonant behavior at the frequency determined by the force constant for motion along $\hat{x}$, namely $\omega_x = \sqrt{k_x/m}$. Only the magnetically induced component of motion is sensitive to the restoring force in the orthogonal direction along $\hat{z}$. Consequently, it peaks at $\omega_z = \sqrt{k_z/m}$. The motions along $\hat{x}$ and $\hat{z}$ are coupled, however, and energy transfer between these two degrees of freedom furnishes an enhancement mechanism that intensifies magnetic effects. Reduction of the classical model to a complex Mathieu equation shows that parametric oscillation of charge motion driven by light gives rise to intense optical magnetism transverse to the axis of propagation. An important conclusion based on the stability diagram of moderately intense optical interactions (Fig. 6) is that parametric resonance enhances magnetic response at virtually any detuning of the incident field.

[1] S. L. Oliveira and S. C. Rand, Phys. Rev. Lett. **98**, 093901 (2007).

[2] S. C. Rand, W. M. Fisher, and S. L. Oliveira, J. Opt. Soc. Am. B **25**, 1106 (2008).

[3] S. C. Rand, J. Opt. Soc. Am. B **26**, B120 (2009).

[4] R. N. Jazar, M. Mahinfalah, N. Mahmoudian, and M. A. Rastgaar, J. Braz. Soc. Mech. Sci. Eng. **XXX**, 182 (2008).

[5] H. A. Lorentz, Teubner (1906).

[6] K. E. Oughstun and R. A. Albanese, J. Opt. Soc. Am. A **23**, 1751 (2006).

[7] C. M. Bender and S. A. Orszag, *Advanced Mathematical Methods for Scientists and Engineers* (McGraw-Hill, New York, 1978).

[8] S. H. Autler and C. H. Townes, Phys. Rev. **100**, 703 (1955).

[9] D. W. Jordan and P. Smith, *Nonlinear Ordinary Differential Equations* (Oxford University Press, Oxford, 2007).

[10] M. Cartmell, *Introduction to Linear, Parametric, and Nonlinear Vibrations* (Chapman and Hall, New York, 1990).

[11] E. I. Butikov, Computing in Science and Engineering **1**, 76 (1999).

[12] D. B. Batchelor, Appl. Phys. Lett. **29**, 280 (1976).

[13] L. D. Landau, E. M. Lifshitz, and L. P. Pitaevskii, *Electrodynamics of Continuous Media* (Pergamon Press, Oxford, 1984).